



# Surface Treatment for Improving Selected Physical and Functional Properties of Tools and Machine Parts—A Review

Daniel Tobała \*, Janusz Kalisz, Kazimierz Czechowski, Iwona Wronska and Zbigniew Machynia

LUKASIEWICZ Research Network—Institute of Advanced Manufacturing Technology, Wrocławska 37a, 30-011 Krakow, Poland; janusz.kalisz@ios.krakow.pl (J.K.); kazimierz.czechowski@ios.krakow.pl (K.C.); iwona.wronska@ios.krakow.pl (I.W.); zbigniew.machynia@ios.krakow.pl (Z.M.)

\* Corresponding author: daniel.tobolal@ios.krakow.pl

Submitted: 20 January 2020 | Accepted: 25 May 2020 | Published: 31 May 2020

**Abstract** Wear resistance, which is one of the main technological quality features of machine parts and tools, is determined by the properties of their surface layer. The demand for high-quality products forces manufacturers to use modern structural and tooling materials as well as efficient and cost-effective methods of their treatment. The paper presents the results of research on selected properties of tools made of tool steels and sintered carbides, as well as parts made of aluminum alloy subjected to selected surface treatment processes, such as mechanical (grinding, turning, milling, burnishing) and thermo-chemical (nitriding, sulfonitriding) processes, and physical vapor deposition (PVD) of coatings. The presented results, including analyses of the surface geometric structure, microstructure, and microhardness, as well as tribological and machining properties of selected materials, indicate the possibility of improving the functional quality of tools and machine parts.

**Keywords** surface layer; coating; wear resistance; tool steel; cemented carbides; aluminium alloy; thermo-chemical treatment

**How to cite:** Tobała, D.; Kalisz, J.; Czechowski, K.; Wronska, I.; Machynia, Z. Surface Treatment for Improving Selected Physical and Functional Properties of Tools and Machine Parts—A Review. *J. Appl. Mater. Eng.* **2020**, *60*(1), 23–36, doi:10.35995/jame60010003.

© 2020 Open Access. This article is distributed under the terms of the Creative Commons Attribution-ShareAlike 3.0 (CC BY-SA 3.0).

## 1. Introduction

Wear resistance, which is one of the main technological quality features of machine parts and tools, is determined by the properties of their surface layer (SL), which include principally surface roughness and hardness. SL properties are produced, most often, by machining processes, often preceded by heat treatment, and sometimes thermo-chemical

treatment as well as by physical vapor deposition (PVD) of coatings (Toboła et al. 2015; Toboła et al. 2017; Toboła and Kania 2018).

The continuous trends in coating development relate to coatings mostly based on TiAlN and AlCrN nitrides through various types of modifications to their chemical compositions and the conditions of the deposition processes. Modifications of their phase compositions, structures and crystallographic orientations, lead to the formation of coatings with desired properties for specific applications. An example is the introduction into the nitride coating of elements such as vanadium, tungsten and molybdenum, which, during the use of the coatings, cause the formation of Magnéli oxide phases, providing these coatings with lubricating properties. Other developments include the deposition of coatings consisting of nitrides and oxynitrides (e.g. AlCrON) and the formation of nitride coatings based on high-entropy alloys (HEA). Nanostructured multilayer coatings, especially superlattice coatings, show particularly advantageous properties (Angelov et al. 2018), (Hovsepian et al. 2005; Hovsepian et al. 2016), (Lin et al. 2019), (Fallmann et al. 2019), and (Czechowski et al. 2019).

The other SL development considered is burnishing, a treatment which consists of local cold plastic deformation of the workpiece by the force and kinetic interaction of the tool with the worked surface. Burnishing is most often used as a smoothing treatment, the main purpose of which is to reduce the surface's unevenness after the previous treatment (which is most often machining). Strengthening the SL is its additional advantage. Increasing the dimensional and shape accuracy of machine parts by burnishing is achieved by plastic deformation of surface irregularities when using rigid pressure. It depends very much on the accuracy of the treatment preceding burnishing (turning, milling or grinding) (Przybylski 1987), (Kalmegh and Khodke 2017), and (Kalisz 2018).

## 2. Tribological Properties of Aluminium Alloy Surface Layer after Grinding, Polishing and Ball Burnishing

One of the principal attributes of the technological quality of machine parts is their wear resistance—this is dependent on mechanical working processes, often preceded by thermal and sometimes thermo-chemical treatment. Wear is related to the surface roughness and to the hardness of the surface layer. Ball and sliding burnishing distinctly improve the surface integrity, including surface topography, strain hardening index and the distribution and profile of the residual stresses. In particular it causes a decrease in the roughness of the machined surface, strengthening of the surface layer and an acquirement of beneficial compressive internal stresses, thereby giving an increase in wear resistance, ensuring the durability of the fit, the ability to transfer larger surface pressures and an improvement in the fatigue properties of parts (Przybylski 1987). Burnishing can be effective for both hard and soft ferrous and nonferrous materials, including plastics. These positive technological and mechanical effects have been reported for several aluminum alloys (Brostow et al. 2015), and (Kalisz et al. 2017).

In this study, the workpiece material was an EN AW-AlCu4MgSi(A) aluminium alloy in the hardened state T451, of quality guaranteed by the metallurgical certificate 3.1. This alloy is used e.g. for highly stressed construction parts, aerospace parts and equipment, as well as machines and motor vehicle parts (Amdouni et al. 2016). Tables 1 and 2 specify the alloy's chemical composition and mechanical properties. Tables 1 and 2 specify the alloy's chemical composition and the mechanical properties.

The abrasion resistance and dynamic coefficient of friction of the alloy were determined. The sample had been prepared by ball burnishing using a tool with an elastic clamp, while its burnishing part was made of a nitride ceramic.

**Table 1.** Chemical composition of EN AW-AlCu4MgSi(A) alloy

Ti	Si	Fe	Cu	Mn	Mg	Cr	Zn	Ti + Zr	other
0.06	0.64	0.04	4.2	0.95	0.76	0.04	0.17	0.06	0.02

**Table 2.** Mechanical properties of EN AW-AlCu4MgSi(A) alloy

Ultimate tensile strength R <sub>m</sub> [MPa]	Yield stress R <sub>p0.2</sub> [MPa]	Elongation A <sub>5</sub> [%]	Hardness [HB]	Density [g/cm <sup>3</sup> ]
445	292	17	110	2.80

For comparison, samples after grinding and polishing were tested. The abrasive wear resistance was determined by the “ball-on-disc” method with a T-01M mechanical tester. Standards ASTM G 99-0 and ISO 20808:2004 were applied. In the ball-on-disc method, sliding contact is brought about by pushing a ball counter-specimen onto a rotating disc specimen with a constant load. A controlled load  $F_n$  is applied to the ball holder and the friction force is measured continuously during the test with an extensometer. For each test, a new ball was used, or the ball was rotated so that a new surface was in contact with the disc. The ball and disc were previously washed in ethyl alcohol and dried. The tests were carried out without a lubricant at room temperature at 60% relative humidity.

Tribological tests, with load  $F = 1$  N and number of cycles  $N = 10,000$ , ball diameter  $d = 6$  mm, rotation speed  $n = 120$  min<sup>-1</sup>, radius of the sliding circle  $r = 3$  mm, showed a large number of irregular upheavals on the sample surface, localized on both sides of the groove. As it was difficult to estimate the heights of these upheavals and their contribution to the calculation of the wear index, it was decided to modify some test conditions to: load  $F = 0.25$  N and number of cycles  $N = 2000$ .

Wear resistance was determined by the measurement of the profile size of the groove (wear trace) resulting from friction with the ball. The geometry of the groove was measured in four sites on the friction path perimeter, every 90°, transversely to the direction of motion. The measurements, using the contact method, were made on a Micro-Combi-Tester and, subsequently, using a computer program, the groove transverse section area was calculated. The volume wear rate was calculated according to the formula:

$$W_s = \frac{V}{F_n \cdot S} \left[ \frac{\text{mm}^3}{\text{N} \cdot \text{m}} \right] \tag{1}$$

where  $V$  is the volume of the worn material calculated according to the mean size of the groove transverse section area,  $F_n$  is the normal force and  $S$  is the friction path.

Surface topographies resulting from grinding, polishing and burnishing were recorded and 3D roughness parameters (ISO 25178 and EUR 1517 EN) were estimated using a TOPO-01P profilometer with a diamond stylus radius of 2.0 μm.

The roughness parameters obtained are listed in Table 3. The lowest values of the roughness parameters, including the arithmetic mean height of the surface,  $S_a$ , root mean square height of the surface,  $S_q$ , and the maximum height of the surface,  $S_z$ , were all obtained after burnishing.

**Table 3.** Mean values of surface geometrical structure measurement results

Surface treatment	Mean values of roughness parameters						
	S <sub>a</sub> , μm	S <sub>q</sub> , μm	S <sub>z</sub> , μm	S <sub>k</sub> , μm	S <sub>pk</sub> , μm	S <sub>vk</sub> , μm	S <sub>ku</sub>
Grinding	0.270	0.342	3.922	0.801	0.249	0.439	3.96
Polishing	0.112	0.208	3.529	0.288	0.263	0.132	4.40
Burnishing	0.029	0.039	0.486	0.104	0.038	0.032	3.01

Figures 1–3 present the isometric view and examples of roughness profiles after grinding, polishing and burnishing. After grinding, surfaces with specific geometrical features—very sharp peaks and valleys—were obtained. All sharp peak profiles were completely deformed by the ball during burnishing and a very smooth profile was thus generated.

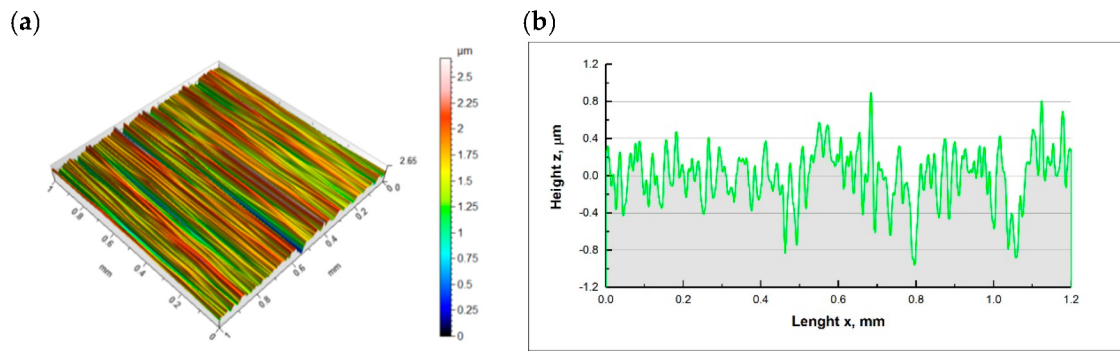


**Figure 1.** Surface characteristics after grinding: (a) isometric view; (b) example of surface profile

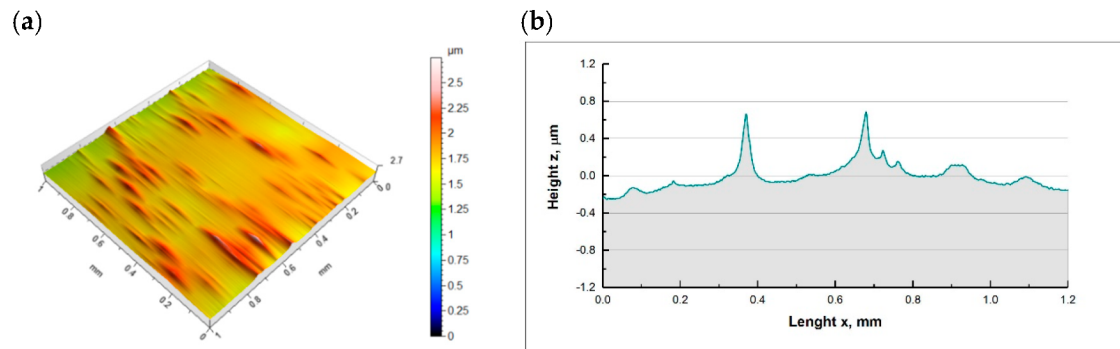


**Figure 2.** Surface characteristics after polishing: (a) isometric view; (b) example of surface profile

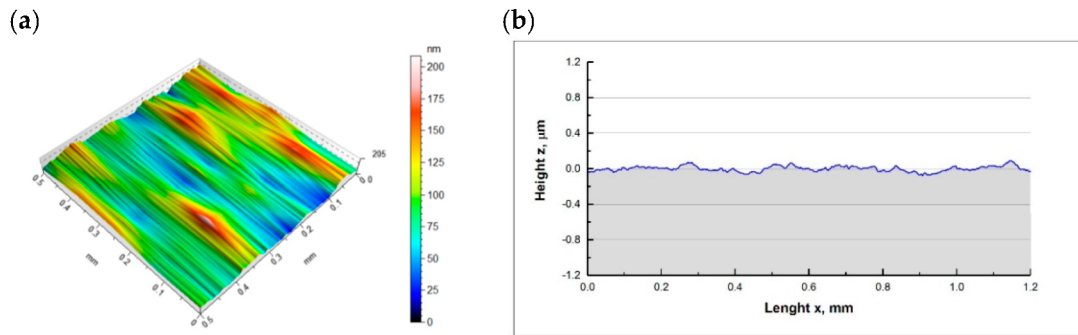


**Figure 3.** Surface characteristics after burnishing: (a) isometric view; (b) example of surface profile

Figure 4 presents the surfaces of samples after wear tests carried out according to the ball-on disc method described above—wear resistance was calculated based on the formula (1). Figure 5 shows a comparison of the dynamic coefficients of friction recorded during wear testing. The average value of the coefficient of friction after rolling burnishing was 0.32 and is lower than the value of this coefficient obtained for the polished surface (0.34) and much lower than for the ground surface (0.45). This indicates a favorable impact of the burnishing process on the tribological property of this aluminum alloy.

Figure 6 compares the volumetric wear rates during wear testing. In comparison with grinding and polishing after burnishing, a more than a two-fold reduction in the volume wear rate was obtained. This confirms the beneficial effect of burnishing on wear resistance of components of this aluminum alloy.

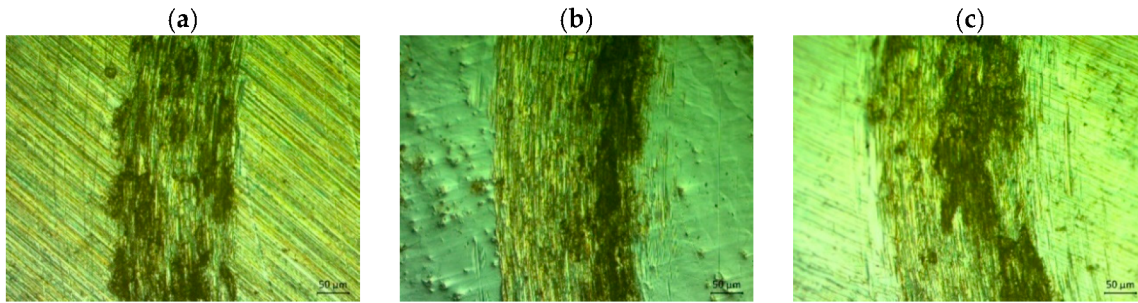


Figure 4. Sample surfaces after wear testing: (a) ground; (b) polished; (c) burnished

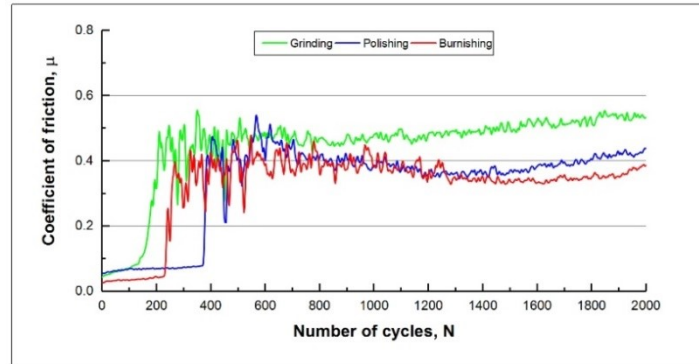


Figure 5. Dynamic friction values for various surface treatments

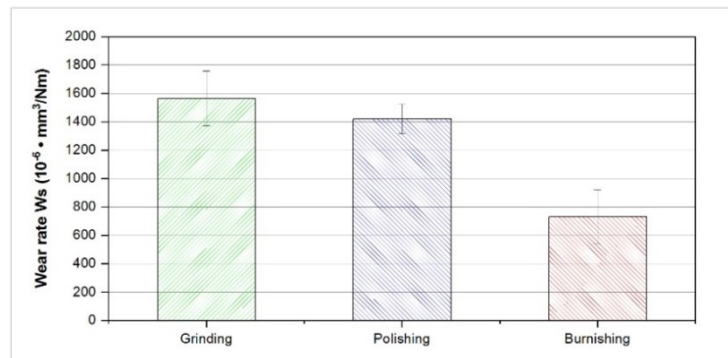


Figure 6. Results of wear rate after various surface treatment processes

### 3. Application of Multilayer Nanostructural Coatings

These dynamically developing techniques for coating deposition on tools with high wear resistance exert a very considerable effect on the economic efficiency of the production process. The economic benefits of coating applications result from an increase in tool lives (lower tool costs) and a greater reliability of the technological process (lower downtimes), as well as from increases in cutting parameters (higher machining efficiency) (Oerlikon-Balzars 2010–2016), (Baptista et al. 2018). For example, only a cutting speed increase of 20%, possibly due to coated tool application, can result in a reduction in costs of 15% per machined component (Bobzin 2017). Coatings for tools can be produced by chemical vapor deposition (CVD) or physical vapor deposition (PVD) methods. CVD, which involves chemical reaction of the gaseous atmosphere components, produces a thin, hard layer on the tool surface. PVD involves depositing thin layers by physical deposition from the gaseous phase, which typically takes place at a significantly reduced pressure of the order of 0.1–1 Pa at temperatures around 300–700 °C. Existing variants of the PVD method in simple cases differ in the method of supplying the heat required to evaporate the deposited material (resistive,



inductive or laser heating, or electron beam bombardment) and, in more complex cases, in the method of obtaining an ionized gaseous phase, i.e. plasma (PAPVD).

One technique of obtaining plasma for PVD is based on the thermal evaporation of a material by electron beam melting and its subsequent ionization (EB-PVD, one of ion plating methods); this technique was widely used at the beginning of the application of PVD, e.g. by the Balzers company, and is still being developed (Oerlikon-Balzers 2010–2016), (Baptista et al. 2018), (Smolik et al. 2018). Plasma can also be obtained by evaporating the metal and ionizing its vapor by a cathodic arc at the site of its formation (PVD arc-plasma method—arc deposition). In the PVD arc-plasma method, cathode material evaporation is effected by high-current arc discharge: continuous (as in the modernized NNW-6.6 equipment of Łukasiewicz-IAMT—Figure 7) or pulsed. Plasma with a high degree of ionization (about 90%) is then produced. The anode is the wall of the vacuum chamber. Targeting and increasing the kinetic energy of ions is achieved by polarizing the substrate on which the coating is applied with a negative voltage (Oerlikon-Balzers 2010–2016), (Czechowski 2017; Czechowski et al. 2019). The high degree of plasma ionization in arc processes distinguishes them significantly from magnetron sputtering and ion plating methods, in which the coatings are partly formed by uncharged molecules. High-energy ions produced in the arc-cathode process lead to higher density coatings at a relatively lower application temperature, as compared to other PVD processes (Sanders and Anders 2000).

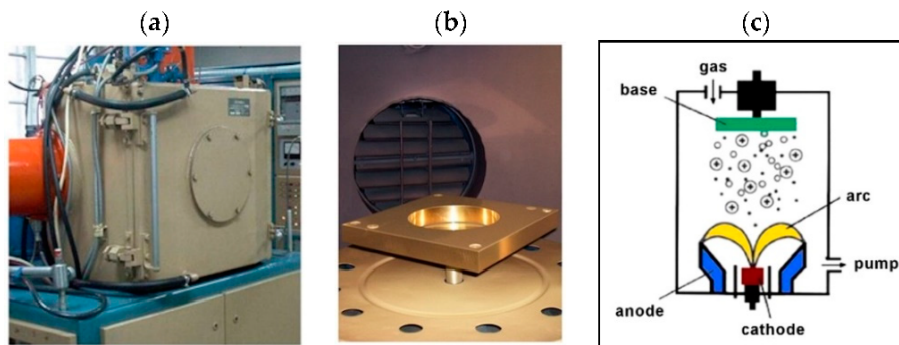


**Figure 7.** View of the chamber (a) of the physical vapor deposition (PVD) arc plasma device at Łukasiewicz-IAMT; inside the chamber—a part with deposited coating (b) and the principle of the device operation (c) (Czechowski 2017)

Due to the structure of coatings deposited on tools, they can be divided into single-layer (monolithic, composite, gradient) and multilayer (microscale, nanoscale, superlattice). These coatings can be of nitrides, carbides, carbo-nitrides, oxides and are multi-component. Multilayered coatings can consist of several, dozens, and even several thousand layers (in the last case a few nm thick). Many layers of the coating give a more favorable stress distribution and better fracture toughness, because the crack energy is dispersed by deflection and branching (Oerlikon-Balzers 2010–2016). Multilayered coatings on the microscale, applied by PVD, consist of several functional layers. They may be (in order from the substrate), e.g. a metallic adhesive layer (e.g. Ti, Cr, Mo, Zr), a basic layer of high hardness and possibly low internal stresses (e.g. TiN, CrN, ZrN, TiCN), a heat blocking layer (e.g. TiAlN, TiZrN) and (on the surface) a layer with a low friction coefficient (e.g. Cr, CrN, TiN) (Panckow et al. 2001). PVD coatings are increasingly being developed as multilayer nanostructured coatings, which provide to tools properties (Oerlikon-Balzers 2010–2016) such as optimum hardness to internal stresses ratios (high tool geometry stability and its uniform wear), higher thermal and chemical resistance (dry machining capability at higher cutting speeds, less groove wear), better sliding properties (improved chip formation, higher quality of processed surface) or greater wear resistance (reduction of tool costs). By selecting the appropriate structure and the specific phase composition of multiphase coatings, their properties can be modified, for example, to increase hardness and reduce the friction coefficient (Panckow et al. 2001).

In Łukasiewicz-IAMT, micro and nano multilayer coatings are developed mainly for cutting tools (including special gear cutting hobs made of high speed steels and cemented carbides, end milling cutters and ball nose endmills

made of cemented carbides and indexable inserts for turning and milling, made of cemented carbides and ceramic materials), as well as for tools for cold working (e.g. punches, dies and other tools made of high speed and tool steels). Anti-wear multilayer coatings developed at Łukasiewicz-IAMT, deposited by arc-plasma PVD, consist of micro- and nanolayer coatings (listed below, from the substrate, to which Ti layer was deposited each time to obtain better adhesion—with a thickness of tens of nm) (Czechowski 2017; Czechowski et al. 2019).

Examples of nanostructured coatings (Czechowski 2017):

- **TiN/(TiAl)N/10x(TiN/(TiAl)N)**—Figure 8—after basic microlayer TiN of about 0.8- $\mu\text{m}$  thick, the (TiAl)N microlayer was deposited, which blocks the heat transfer to the substrate, followed by 10 very thin layers of TiN and (TiAl)N—each with a thickness of about 150 nm—which counteract crack propagation;
- **TiAlCrN/12x(CrN/(TiAl)N)**—Figure 9—after basic microlayer of TiAlCrN approximately 1.5- $\mu\text{m}$  thick (preceded by a 30 nm thick Cr adhesive layer), there are 12 alternate very thin layers of CrN and (TiAl)N (each with a thickness of approximately 60 nm);
- **(TiAl)N/12x((TiAl)N/TiN)**—as a basic microlayer blocking heat flow to the substrate, (TiAl)N was used, followed by 12 very thin, alternatively distributed layers of (TiAl)N and TiN, each having a thickness of approximately 60 nm, which counteract crack propagation;
- **11x(TiN/ZrN)**—11 super-thin alternating TiN and ZrN layers (each with a thickness of 150 nm) are found in this coating.

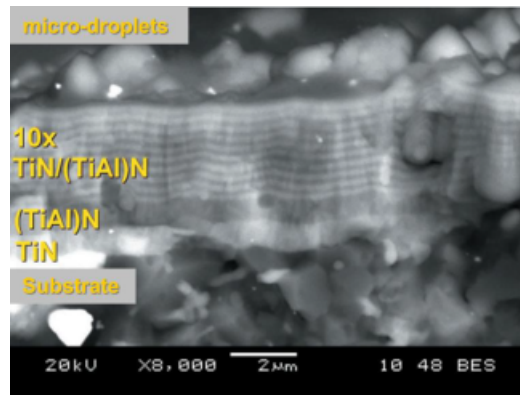


**Figure 8.** Example of structure of multilayer PVD coating of TiN/(TiAl)N/10x(TiN/(TiAl)N) type developed at Łukasiewicz-IAMT, deposited on the cutting edge—SEM micrograph (Czechowski 2017)

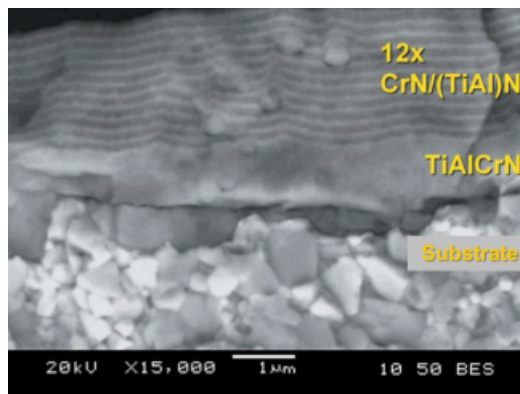


**Figure 9.** Example of structure of multilayer PVD coating of TiAlCrN/12x(CrN/(TiAl)N) type developed at Łukasiewicz-IAMT, deposited on the cutting edge—SEM micrograph (Czechowski 2017)

The microlayer part of the coating is nanostructured, resulting from its production technology. Due to the application of two opposite cathodes, a rotary planetary table and corresponding tooling to provide cyclic shielding, the microlayer is made up of very thin nanolayers, whose thicknesses depend on the PVD process conditions and are

so thin (even of the order of several nm) that they are not visible in the fracture images obtained with a scanning electron microscope (Czechowski 2017; Czechowski et al. 2019).

In order to reveal the structure of the coatings, transverse and tapered low angle ( $5\text{--}6^\circ$ ) metallographic sections were made, which were then observed with a JSM-6460LV scanning electron microscope. The thicknesses of multilayer coatings and individual micro- and nanolayers were measured on micrographs showing fractured coatings (see Figures 8 and 9). The hardness of the coatings and of the substrate was determined on tapered low angle metallographic sections by a Vickers-type digital FM-7 microhardness meter (Future-Tech Corp.) with a force of 0.2452 N. Surface roughness measurements were performed using a Hommel Tester T1000 profilograph (Czechowski 2017).

The hardness of the coatings was 3000–3500 HV0.025, which results in an increase in cutting tool lives when these coatings have been deposited. The research conducted at Łukasiewicz-IAMT demonstrated, during turning of grade 145Cr6 hardened tool steel (with a hardness of about 50 HRC), an increase in tool lives of the cutting edges of cemented carbides after the deposition of multilayer nanostructural coatings, instead of TiN coatings. A good example is the (TiAl)N/12x((TiAl)N/TiN) coating, which produced an up to 2.4-fold increase in tool life compared to the TiN coating. The cutting parameters used were as follows: cutting speed  $v_c = 120$  m/min, feed  $f = 0.07$  mm/rev, depth of cut  $a_p = 0.5$  mm. The SPUN 120308 cutting insert was clamped with a tool rake angle  $\gamma_o = 5^\circ$  and tool cutting edge inclination angle  $\lambda_s = 0^\circ$ .

The deposition of the 11x(TiN/ZrN) coatings, instead of TiN coatings, on blades of a high-speed steel hob with module  $m = 10$  mm (Figure 10), resulted in lower—by about 15%— $VB_{\max}$  values than for TiN-coated cutting edges.



**Figure 10.** High-speed steel hob with multilayer 11x(TiN/ZrN) coating deposited by PVD arc plasma at Łukasiewicz-IAMT—with module  $m = 10$  mm (Czechowski 2017)

In this case, it was more difficult to demonstrate the variation in tool lives of hob cutting edges, due to multilayer coatings, since the differences were not sufficiently great that the number of gear wheels in one cutting hob position could be increased. Therefore, instead of cutting edge lives, the  $VB_{\max}$  flank wear land length values on their surfaces, obtained after the same cutting time, were compared. Due to the variations in the number of teeth on the gear wheels and the machining parameters, the result of the comparison was determined by relative values (Czechowski 2017). After applying the PVD arc plasma coating, the surface roughness of the cutting edge was increased due to the presence of micro-droplets (visible in Figure 8). Their number and size were dependent, to a large extent, on the types of cathode materials and process conditions. The surface roughness parameter  $R_a$  increased 1.5–2 times, but this resulted in only a slight increase in  $R_a$  on the surface of the turned steel (from a few  $R_a$  to less than 40%). The hardness of microdroplets, in which Ti, Zr, Cr and TiAl predominated in this case, was significantly lower than of the nitride coatings of these metals or their alloys—and therefore these droplets were quickly flattened or scratched off the surface of the coated cutting edge (Czechowski 2017).

The work on coatings carried out at Łukasiewicz-IAMT is currently focused on complex nanostructured coatings deposited by the PVD method. The multilayer nature and suitably selected layer sequences will result in very advantageous properties, including significantly higher wear resistance of cutting and cold working tools, especially in difficult working conditions and for high quality surfaces.



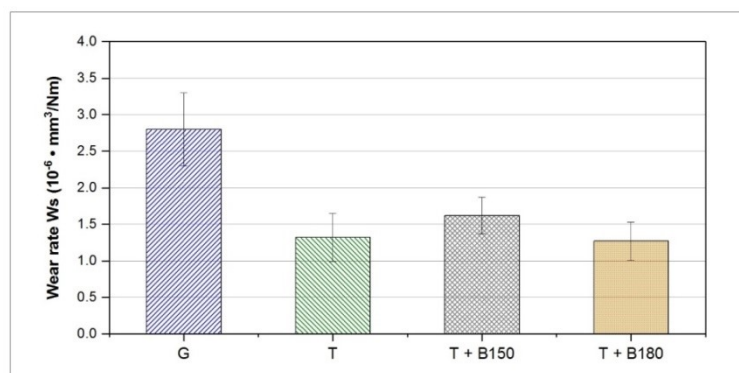
## 4. Selected Processes of Surface Layer Modification of Cold Working Tool Steels

The deterioration of the performance of tools for cold forming generally takes place as a result of progressive tribological wear during operation. Catastrophic (dynamic) wear, which can include chipping of tool edges, which occurs when the ultimate strength is locally exceeded, or fatigue failure in bulk, may be limited by a careful choice of tool material. In some cases, it is necessary to improve the design and technology of the same tools. Tools in processes of cold working are exposed to very high contact stresses during the forming and deformation of the workpiece material. Thus careful preparation of the wearing working surfaces of tools by surface treatment significantly affects their life (Burakowski and Wierzchoń 1995), (Dobrzańska-Danikiewicz 2013), (Dobrzański 2006), (Kula 2000), (Przybylski 1987). The influence of some surface layer modification processes (SLM) on their tribological properties has been analyzed.

The most commonly used mechanical finishing operations of tool steels are turning, milling, grinding, polishing, smoothing and various types of burnishing (rolling and slide burnishing, shot peening) (Oczkoś and Kawalec 2012). The surface topographies after four variants of mechanical processes, with SEM analysis of wear traces after ball-on-disc tests (against two counterparts), for Vanadis 8 tool steel samples with a hardness of  $64 \pm 1$  HRC after heat treatment (HT) are given in Table 4. The tribological test results for both wear rate and dynamic friction are presented in Figures 11 and 12. Details about test parameters are presented in the paper (Toboła et al. 2018).

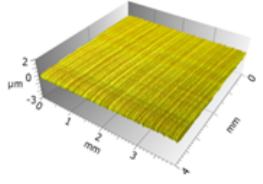
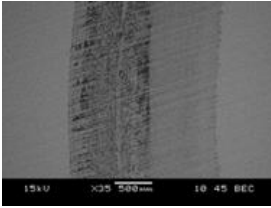
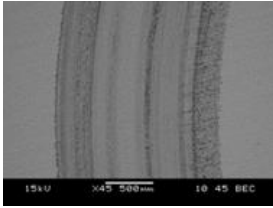
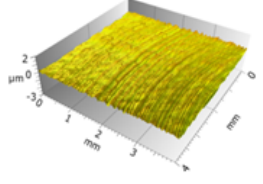
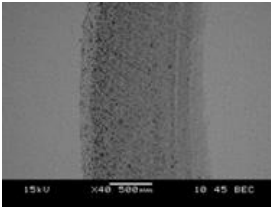
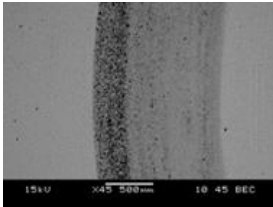
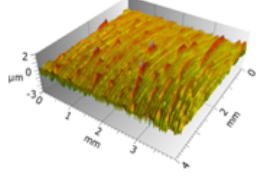
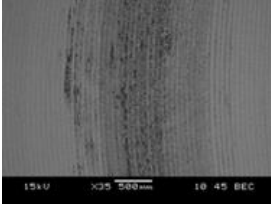
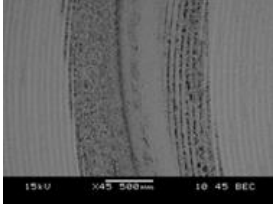
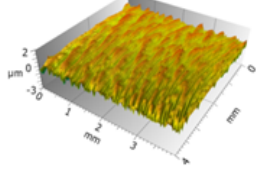
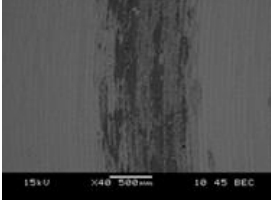
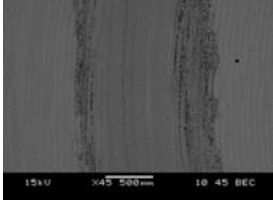
It should also be noted that, among the methods for producing surface layers, especially in industrial practice, thermo-chemical treatments play a dominant role. They include operations enabling changes to the chemical composition and microstructure of workpieces' SL, as a result of changes in temperature and chemical interaction with an appropriate medium.

Thermo-chemical treatment is based on the diffusion change of the chemical composition of SL in order to obtain the required functional properties of tools. SL modification processes include nitriding and sulfonitriding (Baranowska et al. 2007), (Lesz et al. 2010), (Małdziński et al. 2010), (Ratajski et al. 2009), (Cernan et al. 2012), (Sato et al. 2012), (Selg et al. 2013).



**Figure 11.** Wear rates values for Vanadis 8 tool steel samples after mechanical surface treatment processes

**Table 4.** Surface topography with some roughness parameters and images of wear traces after ball-on-disc tests against 100Cr6 and Al<sub>2</sub>O<sub>3</sub> counterparts

Type of mechanical surface treatment	Surface topography	Wear traces after tests against 100Cr6 counterparts	Wear traces after tests against Al <sub>2</sub> O <sub>3</sub> counterparts
HT + Grinding (G)	 $Sa = 0.07 \mu\text{m}$ $Sz = 0.80 \mu\text{m}$		
HT + Turning (T)	 $Sa = 0.09 \mu\text{m}$ $Sz = 1.56 \mu\text{m}$		
HT + T + Burnishing with 150 N force (T + B150)	 $Sa = 0.33 \mu\text{m}$ $Sz = 3.95 \mu\text{m}$		
HT + T + Burnishing with 180 N force (T + B180)	 $Sa = 0.28 \mu\text{m}$ $Sz = 2.46 \mu\text{m}$		

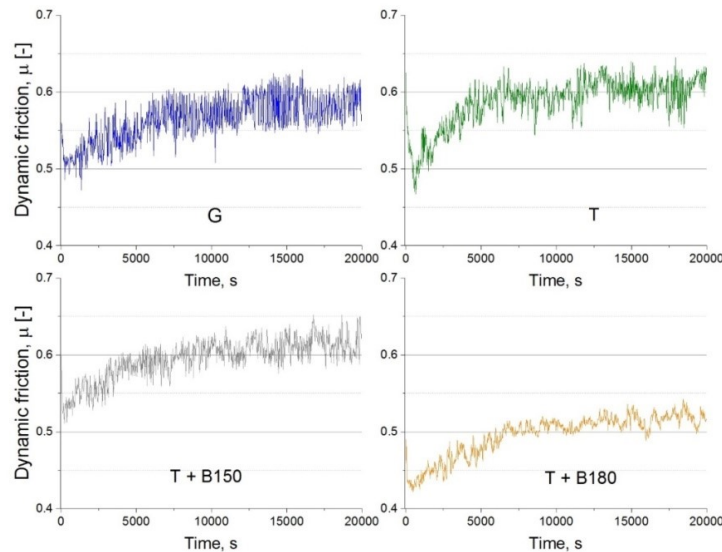


**Figure 12.** Dynamic friction values for Vanadis 8 tool steel samples after mechanical surface treatment processes

Two variants of mechanical processes combined with sulfonitriding treatment were—grinding or hard turning and slide burnishing with 130 N force, respectively. Wear rates determined for Vanadis 8 steel after pin-on-disc tests against 19MnB4 and Al<sub>2</sub>O<sub>3</sub> pins are shown in Figure 13. All the details of the test parameters were presented in an earlier paper (Toboła 2019).

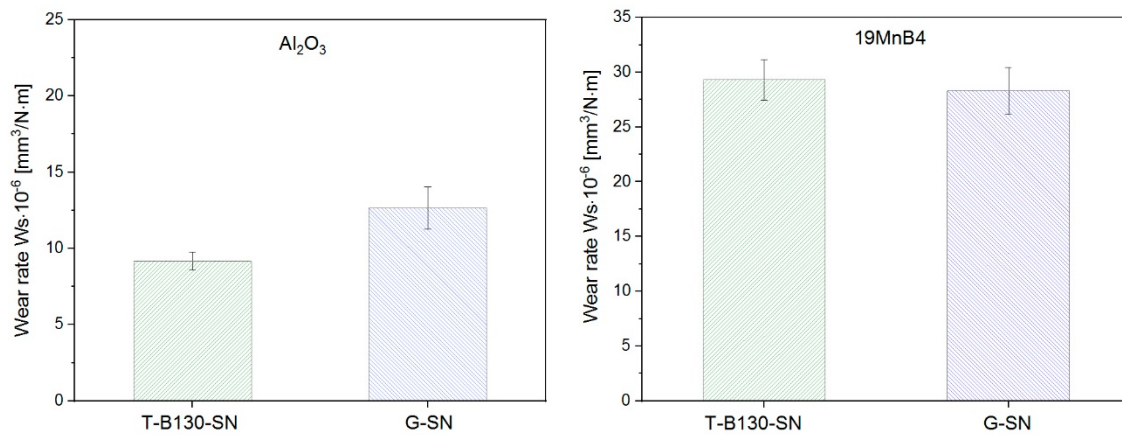


**Figure 13.** Wear rates for Vanadis 8 tool steel samples after mechanical surface treatments combined with sulfonitriding: grinding–sulfonitriding (G–SN) and turning–burnishing with 130 N force–sulfonitriding (T–B130–SN) (Toboła 2019)

About 30% increase in abrasive wear resistance was achieved after the three-stage process compared to grinding–sulfonitriding (G–SN). For 19MnB4 steel pins, however, no significant differences were found of between the wear rates. It should be added that only a slight transfer of pin material on the sample surface occurred after T–B130–SN, as opposed to a much bigger adhesion wear for samples previously ground before sulfonitriding.

## 5. Conclusions

Based on the results presented in this paper, the following conclusions can be formulated:

1. Depending on the type of surface treatment of EN AW-AlCu4MgSi (A) aluminium alloy samples, the average friction coefficients were 0.45 after grinding, 0.34 after polishing and 0.32 after rolling burnishing. Compared to grinding and polishing, wear resistance increased approximately two fold after rolling burnishing;
2. An approximately 2.4-fold increase in the durability of the cutting edges of cemented carbide inserts was achieved by the deposition of the multilayer (TiAl)N<sub>12x</sub>((TiAl)N/TiN) coating, compared to the TiN coating;
3. Approximately 15% less wear on the flank face ( $VB_{max}$ ) for a high-speed steel hob with the 11x(TiN/ZrN) coating compared to the TiN coating was obtained;
4. Further work carried out at Łukasiewicz-IAMT is currently focused on complex multilayer nanostructured coatings deposited by PVD and the development of new sequential processes for the modification of the surface layer of tools and machine parts;
5. A sequential turning and sliding burnishing process can be an alternative to the grinding process for hardened Vanadis 8 tool steel. An over 50% increase in the abrasive wear resistance after sequential turning and burnishing (T + B180) compared to grinding (G) was achieved;
6. The transfer of the counter-sample material (19MnB4 steel) to the surface of samples of Vanadis 8 steel, which was subjected to the T–B130–SN treatment, was several times lower when compared to G–SN. In contrast, a 30% increase in wear resistance (Al<sub>2</sub>O<sub>3</sub> balls) was achieved after using the three-stage process (T–B130–SN), as compared to G–SN.

**Author Contributions:** Conceptualization, D.T.; methodology, D.T., J.K., K.C. and I.W.; formal analysis, Z.M.; investigation, D.T., J.K., K.C., I.W. and Z.M.; writing—original draft preparation, D.T., J.K. and K.C.; review & editing, I.W.; visualization, J.K.; supervision, K.C.

**Funding:** The support from the National Centre for Research and Development of Poland, Warsaw, grant no. LIDER/13/0075/L7/15/NCBR/2016, is gratefully acknowledged for some of the research results included in the article.

**Acknowledgments:** The authors would like to thank all members of the research team involved in the LIDER project: Jolanta Cyboron, Jolanta Laszkiewicz-Lukasik, Aneta Letocha, Sylwester Paweta and Piotr Wyzga.

**Conflicts of Interest:** The authors declare no conflict of interest.

## References

- Amdouni, H., H. Bouzaiene, A. Montagne, M. Nasri, and A. Iost. 2016. Modeling and optimization of a ball-burnished aluminum alloy flat surface with a crossed strategy based on response surface methodology. *International Journal of Advanced Manufacturing Technology* 88 (1–4): 801–14. [CrossRef]
- Angelov, M., T. Cholakova, L. Kolaklieva, R. Kakanakov, and V. Chitanov. 2018. Properties of TiN/CrN superlattice hard coatings deposited by reactive magnetron sputtering. *IOP Conference Series: Materials Science and Engineering* 400: 032001. [CrossRef]
- Baptista, A., F. Silva, J. Porteiro, J. Miguez, and G. Pinto. 2018. Sputtering vapour deposition (PVD) coatings: a critical review on process improvement and market trend demands. *Coatings* 8 (402): 1–22. [CrossRef]
- Baranowska, J., S. E. Franklin, and A. Kochmańska. 2007. Wear behaviour of low temperature gas nitrided austenitic stainless steel in a corrosive liquid environment. *Wear* 263: 669–73. [CrossRef]
- Bobzin, K. 2017. High-performance coatings for cutting tools. *CIRP Journal of Manufacturing Science and Technology* 18: 1–9. [CrossRef]
- Brostow, W., S. Cygan, K. Czechowski, J. Kalisz, J. Laszkiewicz-Lukasik, and A. Letocha. 2015. Tribological properties of (EN AW- $\text{AlCu4MgSi(A)}$ ) aluminium alloy surface layer after ball burnishing. Paper presented at BALTRIB' 2015 VIII International Scientific Conference, Kaunas, Lithuania, November 26–27.
- Burakowski, T., and T. Wierzchoń. 1995. *Inżynieria powierzchni metali*. Warszawa: Wydawnictwa Naukowo-Techniczne.
- Cernan, J., D. Rodzinak, M. Komolik, P. Hvizdos, and K. Semrad. 2012. Tribological properties of sintered steel following plasma nitriding. *Powder Metallurgy Progress* 12 (1): 34–42.
- Czechowski, K. 2017. Effect of nanostructured multilayer coatings on functional properties of tools. *Mechanik* 1: 28–33. [CrossRef]
- Czechowski, K., D. Tobała, and I. Wronska. 2019. Nanostructured multilayer coatings on cemented carbide and high speed steel cutting tools. *Mechanik* 3: 174–78. [CrossRef]
- Dobrzańska-Danikiewicz, A. D. 2013. *Księga technologii krytycznych kształtowania struktury i własności powierzchni materiałów inżynierskich*. Gliwice: International OCSCO World Press.
- Dobrzański, L. A. 2006. Podstawy nauki o materiałach i metaloznawstwo. In *Materiały inżynierskie i projektowanie materiałowe*. Warszawa: Wydawnictwa Naukowo-Techniczne.
- Fallmann, M., Z. Chen, Z. L. Zhang, P. H. Mayrhofer, and M. Bartosik. 2019. Mechanical properties and epitaxial growth of TiN/AlN superlattices. *Surface and Coatings Technology* 375: 1–7. [CrossRef]

- Hovsepian, P. E., D. B. Lewis, Q. Luo, and A. Farinotti. 2005. Corrosion resistance of CrN/NbN superlattice coatings grown by various physical vapour deposition techniques. *Thin Solid Films* 488: 1–8. [CrossRef]
- Hovsepian, P. E., A. P. Ehiasarian, P. Yashodhan, A. A. Sugumaran, T. Marriott, and I. Khan. 2016. Development of superlattice CrNNbN coatings for joint replacements deposited by High Power Impulse Magnetron Sputtering. *Journal of Materials Science: Materials in Medicine* 27 (9): 147. [PubMed]
- Kalisz, J. 2018. Tribological properties of aluminium alloy surface layer after finishing treatments. *Mechanik* 7: 492–95. [CrossRef]
- Kalisz, J., K. Żak, W. Grzesik, and K. Czechowski. 2017. Properties of the subsurface layer after rolling burnishing of an initially milled aluminium alloy. *Journal of Machine Engineering* 17 (3): 66–74.
- Kalmegh, A. P., and P. M. Khodke. 2017. Review on low plasticity burnishing process: A potential for improving mechanical properties of material. *International Journal of Mechanical Engineering and Technology* 8 (5): 791–810.
- Kula, P. 2000. *Inżynieria warstwy wierzchniej*. Łódź: Wydawnictwo Politechniki Łódzkiej.
- Lesz, S., E. Kalinowska-Ozgowicz, K. Gołombek, and M. Kleczka. 2010. Structure and properties of surface layers of selected constructional steels after sulfonitriding. *Archives of Materials Science and Engineering* 42: 21–28.
- Lin, J., X. Zhang, F. Ge, and F. Huang. 2019. Thick CrN/AlN superlattice coatings deposited by hot filament assisted HiPIMS for solid particle erosion and high temperature wear resistance. *Surface and Coatings Technology* 377: 124922. [CrossRef]
- Mądziński, L., M. Bazel, M. Korecki, A. Miliszewski, and T. Przygowski. 2010. Przemysłowe zastosowania azotowania gazowego metodą “ZeroFlow”. *Inżynieria Powierzchni* 3: 48–54.
- Oczoś, K., and A. Kawalec. 2012. *Kształtowanie metali lekkich*. Warszawa: Wydawnictwo Naukowe PWN.
- Company information materials: Oerlikon-Balzers, Ionbond, Platit, CemeCon, Hauzer, SHM, Gühring, VUHZ. 2010–2016.
- Panckow, A. N., J. Steffenhagen, B. Wegener, L. Dübner, and F. Lierath. 2001. Application of a novel vacuum-arc ion-plating technology for the design of advanced wear resistant coatings. *Surface and Coatings Technology* 138 (1): 71–73. [CrossRef]
- Przybylski, W. 1987. *Technologia obróbki nagniataniem*. Warszawa: Wydawnictwa Naukowo-Techniczne.
- Ratajski, J., R. Olik, T. Suszko, J. Dobrodziej, J. Michalski, and A. Gilewicz. 2009. Precise formation the phase composition and the thickness of nitrided layers. *Journal of Achievements in Materials and Manufacturing Engineering* 37/2: 675–89.
- Sanders, D. M., and A. Anders. 2000. Review of cathodic arc deposition technology at the start of the new millennium. *Surface and Coatings Technology* 133–34 (1): 78–90. [CrossRef]
- Sato, S., Y. Arai, N. Yamashita, A. Kojyo, K. Kodama, N. Ohtsu, Y. Okamoto, and K. Wagatsuma. 2012. Surface-nitriding treatment of steels using microwave-induced nitrogen plasma at atmospheric pressure. *Applied Surface Science* 258: 7574–80. [CrossRef]
- Selg, H., S. R. Meka, M. Kachel, R. E. Schacherl, T. Waldenmaier, and E. J. Mittemeijer. 2013. Nitriding behavior of maraging steel: experiments and modeling. *Journal of Materials Science* 48: 4321–35. [CrossRef]
- Smolik, J., A. Mazurkiewicz, R. Brudnias, and A. Piasek. 2018. Complex coatings obtained by a two source beam evaporation. *Journal of Machine Construction and Maintenance* 109 (2): 61–72.



- 
- Toboła, D. 2019. Impact of Mechanical Processes as a Pre-Sulphonitriding Treatment on Tribology Properties of Selected P/M Tool Steels. *Materials* 12: 3431. [CrossRef] [PubMed]
- Toboła, D., W. Brostow, K. Czechowski, P. Rusek, and I. Wronska. 2015. Structure and properties of burnished and nitride AISI D2 tool steel. *Materials Science-Medžiagotyra* 21: 511–16.
- Toboła, D., W. Brostow, K. Czechowski, and P. Rusek. 2017. Improvement of wear resistance of some cold working tool steels. *Wear* 382–83: 29–39.
- Toboła, D., and B. Kania. 2018. Phase composition and stress state in the surface layers of burnished and gas nitrided Sverker 21 and Vanadis 6 tool steels. *Surface and Coatings Technology* 353: 105–15. [CrossRef]
- Toboła, D., J. Cyboron, A. Lętocha, and P. Wyzga. 2018. Wear and friction of hardened P/M tool steels after selected mechanical processes of surface layer modification. Paper presented at 18th Nordic Symposium on Tribology—NORDTRIB 2018, Uppsala University, Uppsala, Sweden, June 18–21.